Fermilab Library
0 1160 0038833 4

Reprinted from
Proceedings of the Intern. Conf.
on High Energy Accelerators and
Instrumentation - CERN 1959

MURA 546

COMPUTATIONAL RESULTS PERTAINING TO USE OF A TIME-DEPENDENT MAGNETIC FIELD PERTURBATION TO IMPLEMENT INJECTION OR EXTRACTION IN A FFAG SYNCHROTRON

L. J. Laslett (*) **and K. R. Symon** (**)

Midwestern Universities Research Association Madison, Wis. (***)

(presented by F. T. Cole)

I. MOTIVATION

In the design of circular accelerators it is often of very great importance to inject efficiently if satisfactory performance is to be achieved, and this aspect of the design certainly warrants explicit attention in consideration of FFAG synchrotrons [1-3] intended for the production of very high current beams [2, 4, 5]. Many of the considerations which apply to the injection process also apply to certain extraction problems, since what is basically involved is an orderly transfer of phase space between regions exterior and interior to the accelerator.

In the present paper we direct our attention to a simplified problem which may be considered as the idealization of a possible method for injection into a fixed-field synchrotron, employing a secularly-changing (decreasing) perturbation of the magnetic field but without the intervention of acceleration mechanisms. It may be mentioned, however, that the specific problem considered here evidently constitutes a rather realistic description, in reverse, of an attractive method of beam *extraction* from a (three-sector) spiral ridge cyclotron in which the aforementioned secular change in effect is achieved by acceleration of the beam into a region of modified magnetic field [6]. With either interpretation, a fundamental feature of the present work is, as we shall see, that the essential non-linear character of the equations of motion is exploited, the dominating non-linear resonance being specifically that for which σ_r, the phase shift per sector of the radial betatron oscillations, approaches $2\pi/3$ in this case.

II. GENERAL DESCRIPTION OF METHOD

As is well known, the inherent non-linear character of the equations for the betatron oscillations in FFAG accelerators can impose very definite limits to the amplitudes of stable oscillations. In cases such that the phase change of the radial betatron oscillations in one sector (σ_r) is near $2\pi/3$, the limitation is primarily controlled by a quadratic term in the equations of motion and the stability limits are then typically indicated by the excursions of unstable equilibrium orbits having a period equal to three sectors. The features of the radial betatron motion are conveniently represented by phase-plots [1, 2, 7], employing as axes the quantities $x \equiv (r-r_0)/r_0$ and $p \equiv dx/d\theta$ with r_0 denoting a reference radius, on which the motion of a particular particle is depicted once per period of the magnet structure to form closed " invariant phase curves " in the stable region. The unstable equilibrium orbits are then represented by fixed points, through which passes the separatrix which bounds the roughly triangular region of stability

(*) Iowa State University, Ames, Iowa.
(**) On leave from the University of Wisconsin, Madison, Wis.
(***) Supported by the United States Atomic Energy Commission.

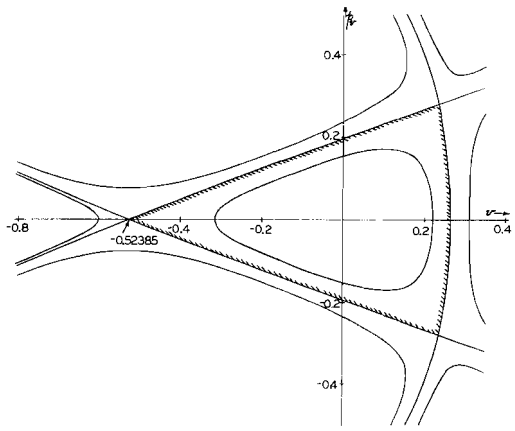

Fig. 1 Phase plot, for $s = 0$ (mod π), of solutions to Eq. (5) with $\nu_r/N = 0.3$ and $B = 1.15$.

(*cf.* Fig. 1, in which conveniently scaled coordinates are used) (*).

In the case which will be of interest here we shall impose a field perturbation, whose wavelength is equal to three periods of the magnet structure, suitably phased so as to " open up " the phase plot in the region of one of the unstable fixed points. The invariant curves which pass through the other two fixed points then no longer intersect at the first fixed point and a separate separatrix serves to define such stable area as may still remain when the perturbation is not too large (Fig. 2). A region of phase space is thus created within which the phase points move through substantially the entire region just outside the stable area. If the stable region is now caused to grow, as a result of decreasing the magnitude of the perturbation, phase points may be expected to be transferred to the interior of the stable region with the same density as initially is present outside.

It is attractive, then, to consider the application of a perturbation which initially is more than sufficiently large to cause the stable region to disappear completely and which is steadily decreased to create a region of stability which ultimately becomes that of the unperturbed accelerator. By an appropriately located injector, particles may now be caused to " flood " the boundary region which surrounds the stable area as it is created and one may expect thereby to fill this area with a phase density equal to that available from the injector. For *efficient* injection it would be desirable, of course, to inject only into that region of phase space from which particles will be captured. It would be convenient, moreover, if this region which must be covered by the injector were to behave in a sufficiently orderly way as to obviate the need to change the direction of the injected beam in accordance with an elaborate program synchronized with the changing strength of the magnetic-field perturbation. In some cases, however, the *area* of phase space which the injector can cover may be sufficiently great as not to be a fundamental limitation, although the phase *density* which it can provide should be used efficiently, and in such cases a programmed scan would either be unnecessary or, at worst, not critical.

To examine the performance which could be achieved by this method in any particular case, a natural initial step is the determination of the phase plots associated with static perturbations representative of the time-dependent perturbation which it is intended to apply. Useful orientation in simple cases can be obtained at this point by analytic means although, of course, computer studies can be helpful.

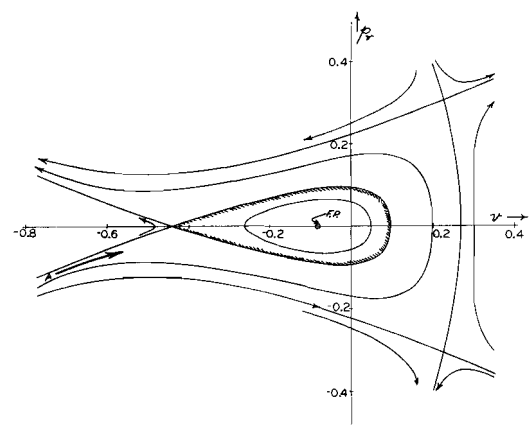

Fig. 2 Phase plot, for $s = 0$ (mod 3π), of solutions to Eq. (6) with $\nu_r/N = 0.3$, $B = 1.15$, and $\lambda = 0.006$. The curves through the upper and lower fixed points are seen to " open up " in the neighborhood of the unstable fixed point situated at $v = -0.44345$, the stable region (shaded) has become smaller than for $\lambda = 0$ (fig. 1), and the stable fixed point has shifted to $v = 0.0838$. The heavy arrow at A suggests a region from which injected particles would flow to flood the boundaries of the stable region.

(*) In this discussion we have tacitly assumed the existence of the so called " invariant phase curves ", although actually over long intervals of time the motion may be found to show a considerable departure from such regular motion and, similarly, the boundary between " stable " and " unstable " regions becomes imprecisely defined [8].

One may then proceed with computations in which the time-dependent perturbation is present, to determine the regions of phase space from which particles will be captured at various stages of the process. If these regions can be caused to fall at locations accessible to an injector system, and if they neither shift about violently nor show more than trivial filamentation, then in principle the proposed method could be said to be practicable. Similarly, such an orderly transferral of phase space could be considered as indicating the potential utility of the inverse process [6] for beam extraction.

In the following sections we describe the results obtained in some initial studies of this injection method, the work so far having been confined to analysis and computations [(*)] for equations chosen, for convenience, to be of a rather simple form, but which it is believed should depict the essential features of more exact equations representative of particle motion in a spirally-ridged FFAG accelerator. Also, for reasons of simplicity, the field perturbation is taken to fall linearly to zero and to remain zero thereafter.

III. THE DIFFERENTIAL EQUATIONS EMPLOYED

In the theory of spirally-ridged FFAG accelerators, the radial betatron motion about the stable equilibrium orbit may be conveniently represented by [9]

$$\frac{d^2u}{d\theta^2}+[a+b\cos N\theta]u = \tfrac{1}{2}b_1(\theta)u^2+\ldots, \qquad (1)$$

where u denotes the radial departure from the stable equilibrium orbit, in units of the radius,

$$b \quad = f/w, \text{ and} \qquad (2a)$$

$$b_1(\theta) = -(f/w^2)\sin N\theta\,, \qquad (2b)$$

in terms of the parameters f, w, and N characterizing the accelerator [2,9]. By introducing the scaled variables

$$s = (N/2)\theta+\pi/4 \qquad (3a)$$

$$v = u/w \qquad (3b)$$

Eq. (1) assumes the form

$$\frac{d^2v}{ds^2}+4\left[\frac{a}{N^2}+\frac{f}{wN^2}\sin 2s\right]v-\tfrac{1}{2}\left(\frac{4f}{wN^2}\right)(\cos 2s)v^2 = 0\,. \qquad (4)$$

Although it is possible by a suitable transformation [10,11] to remove the alternating gradient feature of the linear term, we do not believe it necessary to make this transformation explicitly in the present work but may consider the essential features of interest here to be represented by use of the smooth approximation equivalent of this coefficient [1,11]. Therefore, in what follows, we shall take the unperturbed radial motion as represented adequately by

$$\frac{d^2v}{ds^2}+\left(\frac{2\nu_r}{N}\right)^2 v-\frac{B}{2}(\cos 2s)v^2 = 0\,. \qquad (5)$$

The type of perturbation which will be effective in implementing injection by the method previously described will be, in essence, a periodic variation of the field strength along the equilibrium orbit, with a period equal to the length of three magnet sectors. We thus include the perturbation in the differential equation by writing

$$\frac{d^2v}{ds^2}+\left(\frac{2\nu_r}{N}\right)^2 v-\frac{B}{2}(\cos 2s)v^2-\lambda\cos\frac{2s}{3} = 0\,, \qquad (6)$$

where λ serves to measure the strength of the perturbation. Illustrations of coupled motion may be obtained by considering the pair [9,12]

$$\frac{d^2v}{ds^2}+\left(\frac{2\nu_r}{N}\right)^2 v-\frac{B}{2}(\cos 2s)(v^2-y^2)-\lambda\cos\frac{2s}{3} = 0 \qquad (7a)$$

$$\frac{d^2y}{ds^2}+\left(\frac{2\nu_z}{N}\right)^2 y+B(\cos 2s)vy = 0\,, \qquad (7b)$$

which are derivable from a Hamiltonian

$$\mathcal{H} = \frac{p_v^2}{2}+\frac{p_y^2}{2}+2\left(\frac{\nu_r}{N}\right)^2 v^2+2\left(\frac{\nu_z}{N}\right)^2 y^2- -\frac{B}{6}(\cos 2s)v^3+\frac{B}{2}(\cos 2s)vy^2-\lambda v\cos\frac{2s}{3} \qquad (8)$$

(*) The computations were performed with the MURA IBM-704 computer, using programs prepared by J. N. Snyder, now at the University of Illinois, and M. Storm, the present Head of the MURA Computer Section. We are indebted to Dr. Snyder, Mr. Storm, and others associated with the Computer Section, for their invaluable help and continual cooperation during all phases of the computer work.

with y denoting the axial coordinate, in units of the radius, and

$$p_v \equiv dv/ds \tag{9a}$$

$$p_y \equiv dy/ds\,. \tag{9b}$$

It will be observed that as $\nu_r/N \to 1/3$ the stable solutions to Eq. (5) will become increasingly limited by the $2\pi/3$ resonance, in which the betatron oscillations experience a phase change of $2\pi/3$ in progressing through one magnet sector. Similarly, in progressing through one period of the perturbed structure (i.e. through three sectors) the corresponding phase change would approach 2π and the stability limitation for the solution to Eq. (6) could be regarded in this sense as due to an integral resonance. In examining particular examples of solutions to Eqs. (7a, b) we shall, in what follows, specifically employ

$$\nu_r/N = 0.3 \tag{10a}$$

$$\nu_z/N = 0.0992 \tag{10b}$$

$$B = 1.15 \tag{10c}$$

and λ will assume values in the range

$$0 \leq \lambda \leq 0.023\,. \tag{10d}$$

IV. THE SOLUTIONS TO THE RADIAL EQUATION FOR A STATIC PERTURBATION

The solution to Eq. (5)—i.e. of solutions to Eq. (6) with $\lambda = 0$—can be estimated by use of the analytic methods described by J. Moser [13] and the unstable equilibrium orbits alternatively can be obtained rather accurately by substitution of a trial solution and use of harmonic balance (Table I) [14].

The direct application of the Moser procedure in the case $\lambda \neq 0$ is more tedious, since the initial transformation required to eliminate the forcing term $-\lambda \cos 2s/3$ introduces time-dependent AG terms into the coefficient of v, but a similar, somewhat simplified, analytic method can be applied conveniently and moreover, the fixed points again can be estimated quite well by use of harmonic balance (Table II) [15].

TABLE I

Location of unstable fixed points for Eq. (5) at $s = 0$, as obtained (i) by application of the Moser method, through $(\nu/N - 1/3)^2$; (ii) by harmonic balance with terms of argument $2s/3$, $2s$, and $10s/3$; and (iii) computationally

Point	Calc. by Moser method		Calc. with trial function		Computational results	
	v	p_v	v	p_v	v	p_v
1	− 0.5132	0	− 0.5237	0	− 0.5238	0
2 and 3	0.2256	± 0.2667	0.2319	± 0.2783	0.2320	± 0.2789

TABLE II

Location of stable and unstable fixed points for Eq. (6) at $s = 0$, with $\lambda = 0{,}006$

Point	Analytic calc.		Calc. with trial function		Computational results	
	v	p_v	v	p_v	v	p_v
Stable	− 0.08362	0	− 0.083803	0	− 0.083802	0
1	− 0.44855	0	− 0.44336	0	− 0.44345	0
2 and 3	0.2161	± 0.2841	0.22451	± 0.3023	0.22457	± 0.3030

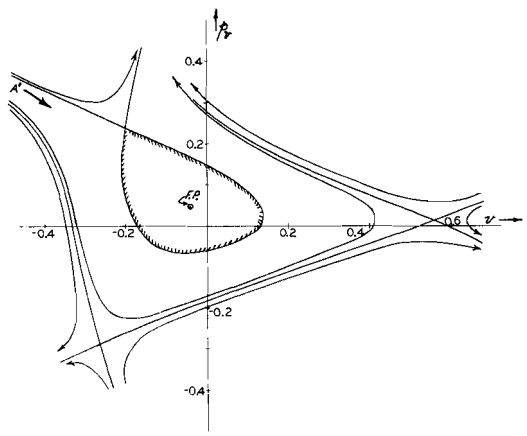

Fig. 3 Phase plot of solutions to Eq. (6), with the same values for the coefficients as were used in Fig. 2 but pertaining to solutions at $s = \pi/2$ (mod 3π).

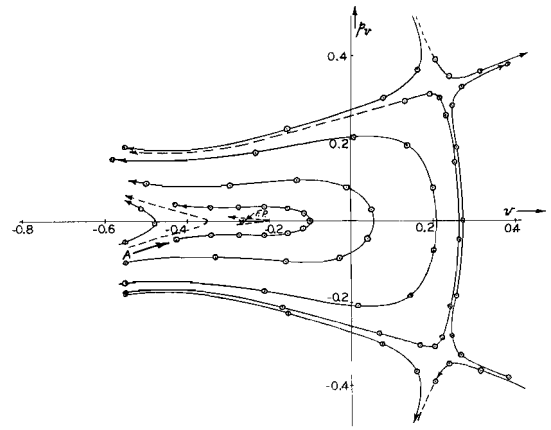

Fig. 5 Phase plot, for $s = 0$ (mod 3π), of solutions to Eq. (6) with $v_r/N = 0.3$ and $B = 1.15$ when λ has the critical value $\lambda_c = 0.01136$. The point designated F.P. represents the confluent fixed point.

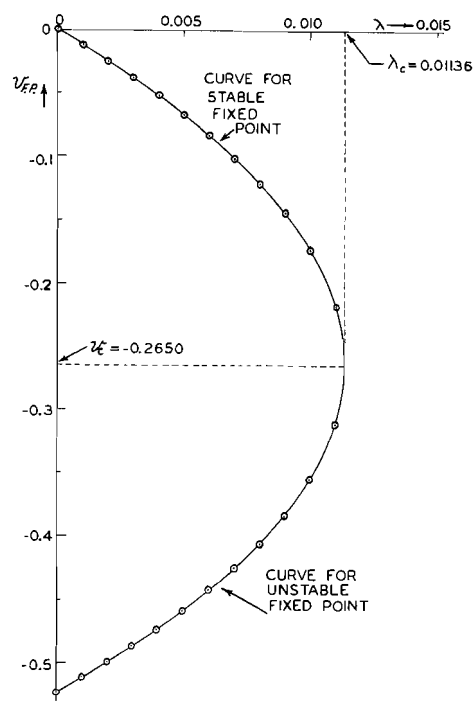

Fig. 4 Coordinates of the stable and unstable fixed points situated on the coordinate axis, for solutions of Eq. (6) with $v_r/N = 0.3$, $B = 1.15$, $s = 0$ (mod 3π) *vs* λ. These two fixed points are seen to approach one another as the strength of the perturbation is increased, becoming coincident when λ assumes the critical value $\lambda_c = 0.01136$.

The detailed characteristics of phase plots which are obtained for any particular value of λ depend, of course, on the particular value of s (mod 3π)—or of θ (mod $6\pi/N$)—to which they apply, but the topological features are independent of s (compare Figs. 2 and 3, which apply respectively to $s = 0$ and to $s = \pi/2$ (mod 3π). Firstly, it is found that, as desired, the application of the perturbation ($\lambda > 0$) does open up the phase curves which originally intersected at one of the unstable fixed points and, secondly, that this fixed point and the stable fixed point approach one another as the strength of the perturbation is increased (Fig. 4), to result in the complete disappearance of the stable region at a critical strength of the perturbation, $\lambda_c = 0.01136$ (Fig. 5).

It may be noted in passing that, for small λ, the locations of these two fixed points which lie on the $p_v = 0$ axis when $s = 0$ (mod 3π) may be estimated by [15]

$$v_1(\lambda) \simeq -\frac{\lambda}{4/9-(2v_r/N)^2} \tag{11a}$$

$$v_2(\lambda) \simeq v_{2,0}+\frac{\lambda}{4/9-(2v_r/N)^2}, \tag{11b}$$

where $v_{2,0}$ denotes the coordinate value of the unstable fixed point when $\lambda = 0$. A parabolic fit, tangent to the lines (11*a*, *b*) at $\lambda = 0$, may be written

$$\lambda = \frac{v\cdot[v-v_{2,0}]}{v_{2,0}}\cdot[4/9-(2v_r/N)^2], \tag{12}$$

for which the maximum value of λ,

$$\lambda_c = [1/9-(v_r/N)^2]\,[-v_{2,0}], \tag{13a}$$

is attained at

$$v_c = \tfrac{1}{2}v_{2,0}. \tag{13b}$$

With $v_r/N = 0.3$ and $-v_{2,0} = 0.5238$, Eqs. (13*a*, *b*) suggest

$$\lambda_c = 0.01106 \qquad (14a)$$

$$v_c = -0.2619\,, \qquad (14b)$$

which may be compared with the computational results

$$\lambda_c = 0.01136 \qquad (14a')$$

$$v_c = -0.2650\,. \qquad (14b')$$

Finally, we note that suitably injected particles —e.g. with their initial phase points lying in the region A of Fig. 2— will move so that their phase points pass completely around the stable region which is formed as the perturbation is being removed. We may expect, therefore, that particles captured in this way will fill the stable region with a phase density equal to the maximum theoretically attainable.

V. INJECTION WITH A SECULARLY-DECREASING PERTURBATION

We imagine the injector situated physically at radii less than those of the stable region into which it is desired to inject—say with $v \leq -0.55$ at $s = 0$ (Fig. 1)—to avoid any interference by the injector with the captured beam. With an assumed particular value for the rate of decrease of the perturbation, one then seeks to find, by digital computations, the regions of phase space within which particles may start, at various initial values of λ, to become captured within the final stable region. The possible difficulties which conceivably could be discovered in such a search would be :

(i) an appreciable fraction of the region of interest might be found not to pass through regions to the left of $v = -0.55$;

(ii) the location of the region with respect to momentum, p_v, might vary strongly with the initial value of λ;

(iii) the region in phase space might be found to be seriously filamented; and

(iv) the coupling between radial and axial motion may be found to play a more dominant role than is usually the case with stable motion, with a consequent complexity of the four-dimentional phase space and of its projections onto the radial and axial sub-spaces.

A. Characteristics when only radial oscillations are present.

For an initial computational investigation it is convenient to confine one's attention to motion in the median plane (axial oscillations absent). One may then commence by finding the range of momenta, p_v, which, at $v = -0.55$ and for various representative initial values of λ, lead to capture into the stability region. From such values other suitable initial conditions could be found by integration backwards in s, to obtain a transformed set of points situated at smaller radii, although with a three-sector accelerator (or with injectors located at every third sector around a larger accelerator) such a reverse transformation should only be carried through a three-sector interval in order to avoid the inclusion of points which would encounter physical interference by the injector structure. The region between these two lines in the radial phase plane—i.e. between the line at $v = -0.55$ and its transform through $\Delta s = 3\pi$—can then be explored to find the boundaries of the regions suitable for injection.

Such a computational survey of the radial phase plane has been made for the case $d\lambda/ds = -0.002/3\pi = -2.122 \times 10^{-4}$, which corresponds to a linear decrease of the perturbation at a rate such that the strength of the perturbation would decrease from its critical value, λ_c, to zero in the time taken by the particle to traverse 17 sectors of the unperturbed machine. The results of this survey are summarized below.

For the initial value $v = -0.55$, the range of "momenta", p_v, within which particles are captured for various initial values of λ, are as shown in Fig. 6. It is noted that the useful values of λ extend consider-

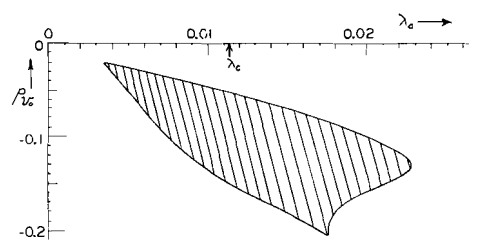

Fig. 6 Range of initial momenta, p_{v_0}, vs. the initial value, λ_0, of λ, for capture of particles into the stable area of Fig. 1 when the initial coordinate is $v_0 = -0.55$. The results were obtained computationally for solutions of Eq. (6) with the perturbation decreased to zero at the rate $\frac{d\lambda}{ds} = -\frac{0.002}{3\pi}$.

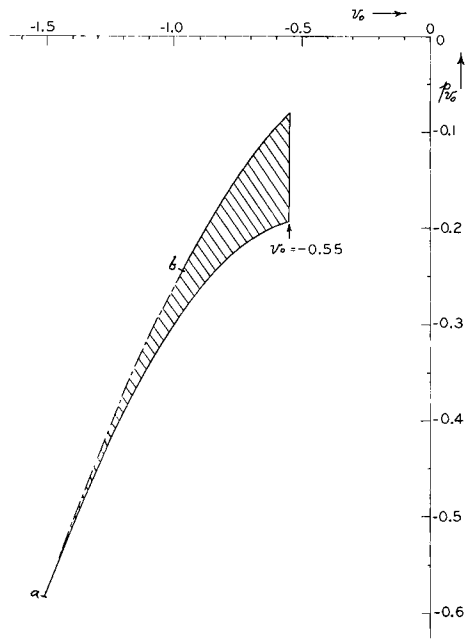

Fig. 7 Range of initial conditions for capture of particles into the stable area of Fig. 1 when the initial strength of the perturbation is $\lambda_0 = 0.0165$ and $\frac{d\lambda}{ds} = -\frac{0.002}{3\pi}$. The boundary *ab* transforms, after three sectors ($\Delta s = 3\pi$), to $v = -0.55$.

ably beyond the critical value, λ_c, since λ will decrease during the time the phase points of the particles progress through the region wherein the stable area is being established. As mentioned above, each such range of values was then projected backward in s to give a second locus of values, applicable three sectors earlier (and for a value of λ greater by 0.002). The intermediate region of the phase plane, between $v = -0.55$ and its transform, was then surveyed to obtain results of which those portrayed in Fig. 7 are typical. For the particular case studied, filamentation of the "phase fluid" was almost entirely absent throughout the entire phase area which was mapped out in this way, although in a few cases the computations appeared to show definite evidence of an incipient filamentation developing along the lower edge of the region (Fig. 8).

The areas of radial phase space which thus should be covered by the injector were obtained from curves of the type shown in Fig. 7. These areas, $A(\lambda)$, have been plotted, vs. the initial value of λ, in Fig. 9 and lead to the integrated result

$$\int A(\lambda)d\lambda = 0.00046. \tag{15}$$

If the injector is capable of delivering n particles per unit area of radial phase space per unit time, the total number of particles which thus could be successfully injected by this means would be

$$\begin{aligned} \mathcal{N} &= \int nA(\lambda)dt \\ &= \frac{n}{|d\lambda/dt|}\int A(\lambda)d\lambda \\ &= \frac{n}{\omega N}\frac{2}{|d\lambda/ds|}\int A(\lambda)d\lambda \\ &= \frac{n}{\omega N}\frac{6\pi}{0.002}0.00046 \\ &= 4.3\frac{n}{\omega N}, \end{aligned} \tag{16}$$

where $\omega \equiv d\theta/dt$ denotes the angular velocity of the particles in the accelerator. This result may be compared with the maximum theoretically obtainable

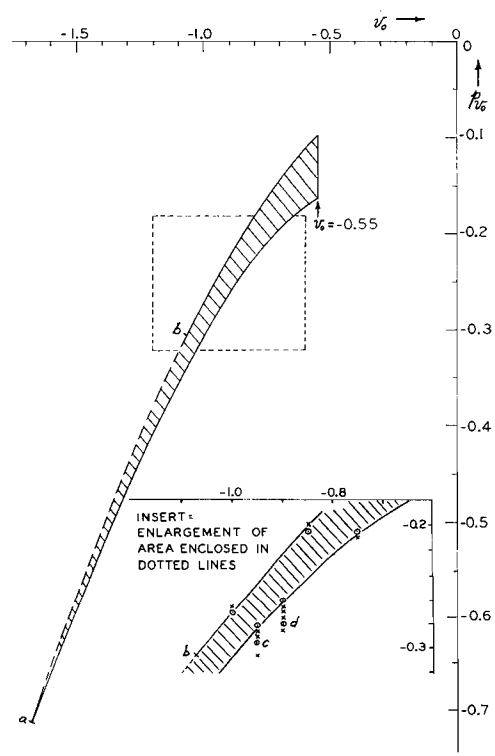

Fig. 8 Detailed portion of diagram, similar to Fig. 7, for capture of particles with $\lambda_0 = 0.0195$. Particles with initial values represented by circles are captured and those depicted by the crossses are not. The boundary *ab* transforms after three sectors to $v = -0.55$. The points denoted by *c* and *d* represent initial values which were found to lead to stable motion and thus provide evidence of incipient filamentation.

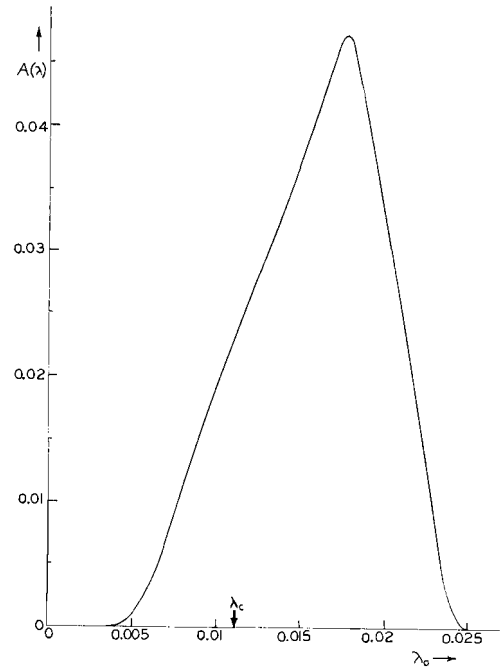

Fig. 9 Area of phase space from which particles may be successfully injected into the stable area of Fig. 1, as a function of λ_0, for $\frac{d\lambda}{ds} = -\frac{0.002}{3\pi}$. The ordinates were obtained from diagrams of the type illustrated in Fig. 7, in which one boundary represented the locus of points which transform after three sectors to $v = -0.55$. From the date shown here, the result $\int A(\lambda)\, d\lambda = 0.00046$ was obtained.

by direct injection, during a three-sector interval, into the stable area without violation of Liouville's theorem, namely

$$\mathcal{N} = \frac{n}{\omega}\left(\frac{6\pi}{N}\right) . \text{[Area of stable phase plot]}$$

$$= \frac{n}{\omega}\left(\frac{6\pi}{N}\right)(0.223)$$

$$= 4.2\,\frac{n}{\omega N} . \qquad (17)$$

It is evident, from comparison of the results (16) and (17), that excellent efficiency of injection into radial phase space has been obtained from the region mapped in this example, although with injection through more than three sectors, or with more complicated differential equations, a more pronounced filamentation of phase space might well develop to present practical difficulties. The transfer of radial phase space from outside the stable region to the interior appears to be quite orderly in the case which we examined and so encourages a continuation of the investigation of this injection (or extraction) method. The exact azimuth at which the injector might best be situated might be adjusted, in practice, to achieve a convenient match to the properties of the injector; it probably would be convenient to select a location where the usable values of p_v vary the least during the interval that the secularly-changing perturbation is being employed and for which the phase diagrams might be similar to that shown in Fig. 10.

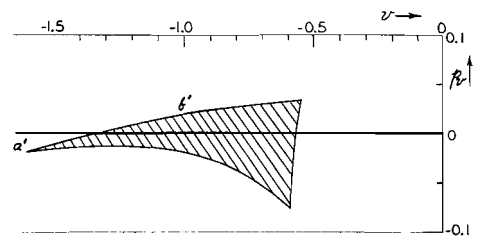

Fig. 10 Transformation of the shaded area depicted in Fig. 7 from $s = 0$ to $s = 3\pi/32$, so that this region becomes more centrally located with respect to $p_v = 0$ (compare Figs. 2 and 3, for which the corresponding values of s differ by $\pi/2$). The segment $a'b'$ of the boundary represents the transformation of the portion denoted as ab on Fig. 7. In either case the shaded region has an area estimated as 0.042 vp_v-units.

B. The effect of axial motion.

As in other accelerator investigations, the inclusion of the additional, axial degree-of-freedom in the present study introduces considerable complication and requires a rather extended amount of computation if a comprehensive picture is to be obtained. The importance of including the axial motion in such studies is clear, however, as has been emphasized by Terwilliger in connection with a computational investigation [16, 17] of a method which proved to afford a promising means of beam *extraction* from a spiral sector accelerator. Basically, this latter work was concerned with the use of a pulsed localized field bump which served to perturb the entire beam into a region of strong d.c. magnetic field, whence it would be bent down the spiral and out of the accelerator. Terwilliger's investigation [16] of combined radial and axial motion indicated considerable phase distortion (and, effectively, loss of phase density) in the unperturbed accelerator if one employed amplitudes comparable with stability limits. Specifically, with a beam for which the oscillation amplitudes were originally about one-half as great as the stability limits, so

that the coupling was not pronounced, and for which the amplitudes each were further damped by a factor of about 7 during the acceleration process, use of the pulsed field was then found to permit orderly *extraction* with high efficiency. The results which we are able to cite at the present time in regard to the inclusion of axial motion in the problem reported here are certainly not sufficiently complete to afford a comprehensive picture—as we shall see, however, the preliminary results which have already been obtained do indicate that, as expected, the axial motion exerts a marked effect on the performance and may detract materially from the utility of the method if efficient *injection into the entire stability region* of the accelerator is required.

A search for the y-stability limit for solutions to Eqs. (7*a*, *b*) in the absence of the perturbation indicated that this limit lay between 0.72 and 0.85 if the amplitude of the radial motion was initially zero (i.e. corresponding to the origin of the radial phase plot shown in Fig. 1). For larger amplitudes the permissible initial axial amplitudes were somewhat reduced, as shown in Table III.

TABLE III

Computational estimates of limiting axial amplitudes, with various initial radial amplitudes, for solutions to Eqs. (7a, b) with $\lambda = 0$

$p_{v_0} = p_{y_0} = 0$

v_0	y_0	
	Stable	Unstable
0	0.72	0.85
− 0.1	0.61	0.72
− 0.25	0.52	0.61

To illustrate the influence of axial motion on the proposed injection method, we have made preliminary computations for the case in which the initial strength of the perturbations is $\lambda_0 = 0.0165$ (and $d\lambda/ds = -0.002/3\pi$) and for which Fig. 7 applies in the absence of axial motion. The y-stability limits for Eqs. (7*a*, *b*) were then sought for $v_0 = -0.55$ and for $v_0 = -0.85$, in each case assigning to the initial radial momentum, p_{v_0}, a value near the center of the previously permissible range of values. The results of this search, summarized in Table IV, indicate that the axial stability limits for these representative cases were materially smaller than those shown in Table III.

TABLE IV

Computational estimates of limiting axial amplitudes, with representative initial conditions for the radial motion, for solutions to Eqs. (7*a*, *b*) with $\lambda_0 = 0.0165$ and $d\lambda/ds = -0.002/3\pi$

$p_{v_0} = 0$

v_0	p_{v_0}	y_0	
		Stable	Unstable
− 0.55	− 0.13625	0.31	0.37
− 0.85	− 0.22	0.19	0.21

Guided by the results shown in Table IV, the range of permissible values of p_{v_0}, leading to stable motion, was then examinaed at $v_0 = -0.55$ and at $v_0 = -0.85$ for several initial axial amplitudes. The results of this survey are summarized in Table V.

TABLE V

Computational estimates of range of permissible radial momenta, with representative initial radial and axial coordinates, for solutions to Eqs. (7*a*, *b*) with $\lambda_0 = 0.0165$ and $d\lambda/ds = -0.002/3\pi$

$p_{y_0} = 0$

y_0	v_0	p_{v_0}			
		Unstable	Stable	Stable	Unstable
0	− 0.55	− 0.0775	− 0.0800	− 0.1925	− 0.1950
0.19		− 0.09	− 0.10	− 0.19	− 0.20
0.22		− 0.09	− 0.10	− 0.19	− 0.20
0.26		− 0.10	− 0.11	− 0.19	− 0.20
0.31		− 0.12	− 0.13	− 0.19	− 0.20
0.37		− 0.14	− 0.15	− 0.20	− 0.21
0.44		− 0.18	− 0.19	− 0.21	− 0.22
0.52		− 0.22	− 0.23	− 0.24	− 0.25
0	− 0.85	− 0.190	− 0.195	− 0.245	− 0.250
0.19		− 0.21	− 0.22	− 0.25	− 0.26
0.22		− 0.22	− 0.23	− 0.26	− 0.27
0.26		− 0.23	− 0.24	− 0.27	− 0.28
0.31		− 0.25	− 0.26	− 0.28	− 0.29

It is clear that axial amplitudes much smaller than those which appear in Table III result in a material reduction of the useful range of p_{v_0}. The larger values of y_0 listed in Table V are seen, moreover, to be associated with values of p_{v_0} differing from those suitable for $y_0 = 0$, and injection with values of y_0 as large as those listed near the end of each section of Table V may be of rather limited utility.

VI. CONCLUSION

The particular injection method discussed in this paper was found to permit efficient transfer of *radial* phase space between regions exterior and interior to the accelerator, although complications might be expected ro arise if the physical limitation imposed at the time the beam returns to the injector azimuth were deferred for longer than the three sectoıs considered here. The results of the method appear to show a close resemblance to those which previously [6] have indicated the potential utility of a similar perturbation for the efficient *extraction* of a beam from a three-sector fixed-field accelerator.

The preliminary studies of the influence of substantial axial oscillation amplitudes on the particle behavior indicated that this influence was pronounced and so might detract materially from the practicality of the method unless additional considerations, such as the limitation of axial amplitudes by the vacuum chamber or the damping of oscillation amplitudes prior to use of the method for *ejection*, served to limit the axial amplitudes to values considerably less than are dynamically stable in the absence of the perturbation.

It is hoped that the method and results reported here will prove suggestive of other possible methods of utilizing a secularly-changing perturbation in conjunction with the non-linear dynamical properties of the orbits, including methods in which the perturbation may have a greater period than that employed here and so would interact with a machine resonance rather than with an inherent sector resonance.

It is a pleasure to acknowledge the assistance of Mr. Seymour J. Wolfson, a MURA summer visitor from Wayne State University, in some of the algebraic and numerical calculations connected with the analytic phases of this investigation, and to thank Mr. Igor Sviatoslavsky for assistance with some of the graphical work.

LIST OF REFERENCES

1. Symon, K. R., Kerst, D. W., Jones, L. W., Laslett, L. J. and Terwilliger, K. M. Fixed-field alternating-gradient particle accelerators. Phys. Rev., *103*, p. 1837-59, 1956.
2. Laslett, L. J. Fixed-field alternating-gradienst accelerators. Science, *124*, p. 781-7, 1956.
3. Kerst, D. W., Symon, K. R., Laslett, L. J., Jones, L. W. and Terwilliger, K. M. Fixed field alternating gradient particle accelerators. CERN Symp. 1956. *1*, p. 32-5.
4. Kerst, D. W., Cole, F. T., Crane, H. R., Jones, L. W., Laslett, L. J., Ohkawa, T., Sessler, A. M., Symon, K. R., Terwilliger, K. M. and Vogt-Nilsen, N. Attainment of very high energy by means of intersecting beams of particles. Phys. Rev., *102*, p. 590-1, 1956.
5. Kerst, D. W. Properties of an intersecting-beam accelerating system. CERN Symp. 1956. *1*, p. 36-9.
6. Blosser, H. G. et al. A proposal for a nuclear research facility in the medium energy range utilizing a 64″ variable energy multiparticle cyclotron. Michigan State University. Department of Physics and Astronomy report. East Lansing, Michigan. 1958. Section III-A.1-C, p. 67-76. (unpublished).
7. Laslett, L. J. and Symon, K. R. Particle orbits in fixed field alternating gradient accelerators. CERN Symp. 1956. *1*, p. 279-89.
8. Moser, J. Nonexistence of integrals for canonical systems of differential equations. Commun. pure appl. Math., *8*, p. 409-36, 1955.
9. Cole, F. T. Mark V FFAG expanded equations of motion. MURA (*) 95. 19 January, 1956.
10. Courant, E. D. and Snyder, H. S. Theory of the alternating-gradient synchrotron. Ann. Phys. New-York, *3*, p. 1-48, 1958. Equations (4.4) and (4.5) on p. 18.
11. Hagedorn, R., Hine, M. G. N. and Schoch, A. Non-linear orbit problems in synchrotrons. CERN Symp. 1956. *1*, p. 237-53.
12. Hagedorn, R. Note on an instability on a difference resonance line. CERN Symp. 1956. *1*, p. 293-4.
13. Moser, J. Stabilitätsverhalten Kanonischer Differentialgleichungssysteme. Nachr. Akad. Wiss. Göttingen. Math. Phys. Kl. 1955. p. 87-120.
14. Laslett, L. J. Concerning the $\nu/N \rightarrow 1/3$ resonance. 1. Application of a variational procedure and of the Moser method to the equation $d^2v/dt^2+(2\nu/N)^2v+(1/2)(\sin 2t)v^2=0$. MURA (*) 452. April 13, 1959.
15. Laslett, L. J. and Wolfson, S. J. Concerning the $\nu N \rightarrow 1/3$ resonance. V: Analysis of the equation $d^2v/ds^2 + (2\nu/N)^2v-(b/2)(\cos 2s)v^2 - \lambda \cos(2s/3) = 0$. MURA (*) 497. 1959.
16. Terwilliger, K. M. Beam extraction from an FFAG synchrotron. MURA (*) 427. 1958.
17. Jones, L. W. and Terwilliger, K. M. Beam extraction from FFAG accelerators. See p. 48.

(*) see note on reports p. 696.